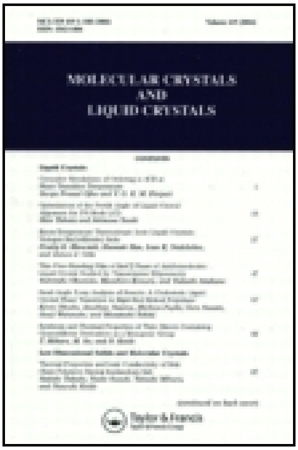

Molecular Crystals and Liquid Crystals
Publication details, including instructions for authors and subscription information:
http://www.tandfonline.com/loi/gmcl16

Light-Scattering Study of Thermotropic Liquid Crystals and Micellar Solutions

M. A. Anisimov [a] , S. A. Konev [a] , V. I. Labko [a] , G. L. Nikolaenko [a] , G. I. Olefirenko [a] & I. K. Yudin [a]
[a] Moscow Oil and Gas Institute, Moscow, B-296, USSR
Version of record first published: 13 Dec 2006.

To cite this article: M. A. Anisimov , S. A. Konev , V. I. Labko , G. L. Nikolaenko , G. I. Olefirenko & I. K. Yudin (1987): Light-Scattering Study of Thermotropic Liquid Crystals and Micellar Solutions, Molecular Crystals and Liquid Crystals, 146:1, 421-434

To link to this article: http://dx.doi.org/10.1080/00268948708071828

Mol. Cryst. Liq. Cryst., 1987, Vol. 146, pp. 421–434

Printed in the United States of America

Light-Scattering Study of Thermotropic Liquid Crystals and Micellar Solutions

M. A. ANISIMOV, S. A. KONEV, V. I. LABKO, G. L. NIKOLAENKO,
G. I. OLEFIRENKO and I. K. YUDIN

Moscow Oil and Gas Institute, Moscow B-296, USSR

(*Received January 6, 1987*)

The accurate dynamic and static light-scattering study of pretransitional phenomena in the isotropic phase of liquid crystals and in the micellar phase of amphiphilic solutions was carried out. It was shown that the existence of the smectic ordering affects the susceptibility behaviour in the isotropic phase. In the vicinity of the micellar solution critical point there is a single characteristic length as well as in ordinary binary mixtures in spite of the large polydispersity of the amphiphilic molecules.

Keywords: light-scattering, nematic-isotropic transition

I. INTRODUCTION

Great progress in the study of phase transitions and critical phenomena has taken place over the last twenty years. Nevertheless there are some unsolved problems for the more complicated systems (thermotropic and lyotropic liquid crystals, micellar solutions, microemulsions etc.). Moreover, in the study of the nature of such systems these problems appear to be key ones both in theoretical and experimental aspects.

Among disputable problems there is the critical behaviour of the susceptibility in the isotropic phase of liquid crystals. A generally accepted description of the isotropic–nematic (I–N) transition is based on the Landau–de Gennes mean-field phenomenological theory[1,2] with the nematic order fluctuation corrections in the Gaussian approximation. Mean-field theory predicts the Curie-Weiss law for the susceptibility:

$$\chi \sim (T - T^*)^{-1} \tag{1}$$

where T^* is the temperature of the absolute stability limit of the isotropic phase. The departures from the Curie-Weiss law are observed systematically in the vicinity of T_{IN}.[3,4] These departures are manifested usually by a bending down of the curve $\chi^{-1}(T)$. The breakdown of the $(T - T^*)^{-1}$ type behaviour close to T_{IN} has been demonstrated on a large number of samples and techniques, in spite of some definite quantitative discrepancies regarding the amplitudes of these departures and the corresponding crossover temperature region.

It is possible to explain the observed anomalies by the fluctuations correction term connected with the third-order term in the Landau–de Gennes expansion.[5,6] Note, however, that some studies of series of smectogenic liquid crystals showed that the above mentioned departures are enhanced by the nearness of the smectic phase.[7,8] Zink and de Jeu[9] argued recently on the basis of their light-scattering study in nCB series that there was no correlation between the departures from the $(T - T^*)^{-1}$ law and the existence of the smectic-A phase. However, the interpretation of their results is doubtful because of the narrow investigated temperature range and insufficient accuracy of their measurements. In view of this result it was interesting to carry out the light-scattering measurements in a mixture of two liquid crystals.[10] One component should have only the isotropic–smectic-A phase transition (I–A) while the other should have the isotropic–nematic one. Thus the possible even-odd effects would be eliminated. Very accurate light-scattering measurements by Gohin[8] in n04 series and ours[10] in the mixtures $\overline{6}0\overline{1}\overline{0}/\overline{6}0\overline{6}NO_2$ demonstrated the correlation between the departures from the $(T - T^*)^{-1}$ law and the proximity of smectic-A phase. This effect was interpreted in terms of a coupling between the fluctuations of the transitional and orientational order.[11,12] According to these works the nematic susceptibility in the isotropic phase is given by

$$\chi^{-1} = a\frac{T - T^*_{IN}}{T^*_{IN}} + \frac{C_{NS}T^{*\,1/2}_{IS}}{(T - T^*_{IS})^{1/2}} - \frac{B^2_{NS}T^{*\,3/2}_{IS}}{(T - T^*_{IS})^{3/2}} \tag{2}$$

where T^*_{IN}, T^*_{IS} are the bare (in the absence of the nematic–smectic coupling) absolute stability limits of the isotropic phase for I–N and I–S transitions correspondingly, C_{NS} and B_{NS} are proportional to the nematic–smectic coupling constants.

We carried out the precision measurements of the light-scattering in several liquid crystals and their mixtures in the wide temperature range. Results of our study show evidently that the isotropic susceptibility behaviour depends upon the existence and nearness of the smectic phase.

We also investigated static and dynamic light-scattering in nonionogenic micellar solution, which has a low critical consolution point. It was shown that in spite of the large polydispersity of the amphiphilic molecules there exists a single critical length as in ordinary binary mixtures.

Technique

Two almost identical experimental setups are used for investigations in liquid crystals and micellar solution. The scheme of the photometer is presented in Figure 1. The beam of He–Ne laser is focused in the center of the cylindrical cell by a lens L_1 with focal length of 15 cm. The scattered light is collected at angle θ with a photomultiplier (PMT) which is fixed on the arm of the goniometer. The PMT is

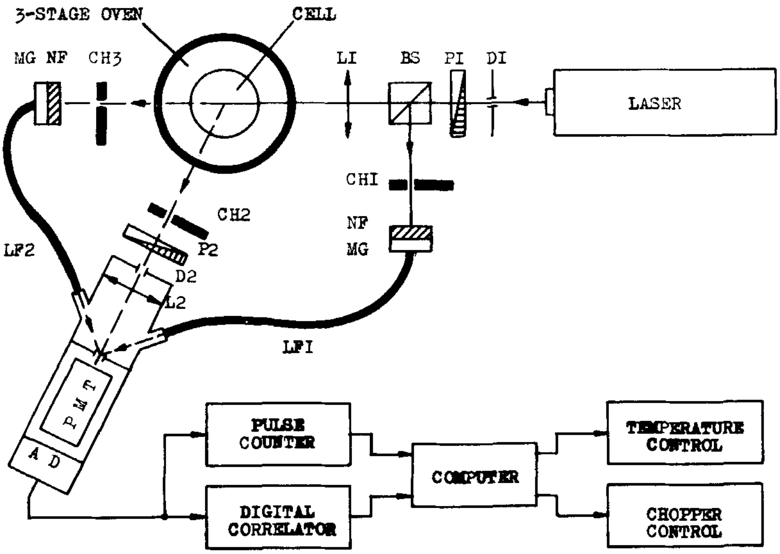

FIGURE 1 Scheme of the photometer.

closed by a metal tube housing. The pinholes D_2, D_3 and the lens L_2 form the scattering volume image on the photocathode. The polarizations of incident and scattered beams are established by means of the polaroids P_1 and P_2. Two light fibers (LF_1 and LF_2) transmit the passed laser beam as well as the fraction of the incident one on to the PMT photocathode. Required attenuation and spatial averaging of these beams are performed by neutral glass filters and milk glasses. Three choppers control the light beams in accordance with the experimental conditions. The photon counting system and digital correlator operate with the microcomputer online. The photon counting system consists of PMT, amplitude discriminator AD and one-board pulse counter. This system has the following parameters: linearity up to $2 \cdot 10^6$ pulse/s better than 0.2%, dark counting ~3 pulse/s. A 4-bit correlator built by us has 128 channels, sample times from 100 ns to 10 s, a post computational delay of 0–2047 channels before last 8 channels, and an original system of "dust cuttoff."

The cell was located within a three-stage temperature controlled oven. The temperature sensitive element was a copper-manganin bridge placed on the internal copper block with the balance temperature 0°C. The external block was water-cooled. The cell temperature could be raised up to 160°C. It could be stabilized with an accuracy of 0, 2 mK. The temperature was measured by means of a platinum resistor placed in the internal copper block. The measurements of light-scattering intensity, depolarization ratio, turbidity and autocorrelation function, the photometer and temperature control, as well as the data processing were performed by the microcomputer.

Cylindrical cells used were made of optical pyrex glass (internal diameter 1.2 cm and 0.3 cm, height 3 cm). All sample manipulations were performed in a box with dry nitrogen. The dry cell was filled with liquid crystal through a micropore membrane filter (pore size 0.22 μm). The dissolved air was evacuated, then this cell was corked by a closely fitting teflon plug. The micellar solution preparation differed from that described in Ref. 13 with the preliminary filtration of an amphiphile and the soldering of the cells.

Results of liquid crystal study

The results of our study of liquid crystals are represented in the Table I. The phase diagrams of the mixtures $\overline{6}O\overline{8}/\overline{6}O\overline{10}$ and $\overline{6}O\overline{10}/\overline{6}O\overline{6}NO_2$ are shown in Figure 2. The measured value was the relative light-scat-

LIQUID CRYSTALS		PARAMETERS				
		$T_{IN}(T_{IA})$°C	T_{NS} °C	$T_{IN}-T_{NS}$	γ_W[1]	γ_A[1]
BMOAB		73.72	NO	-	0.99	0.82±0.02
$\overline{6}O\overline{8}$		89.06	65.46[2]	23.60	0.93	0.72±0.03
$\overline{6}O\overline{8}/\overline{6}O\overline{10}$ (32.6% $\overline{6}O\overline{10}$)		88.98	71.62[3]	17.36	0.91	0.70±0.03
$\overline{6}O\overline{10}$		88.93	83.18	5.75	0.87	0.69±0.03
$\overline{8}CB$		41.09	35.49	5.60	0.90	0.68±0.03
$\overline{9}CB$		49.70	47.82	1.88	0.88	0.50±0.05
$\overline{6}O\overline{6}NO_2$		(69.99)	NO	-	0.78	0.61±0.04
Mix. $\overline{6}O\overline{10}/\overline{6}O\overline{6}NO_2$ Mol.% $\overline{6}O\overline{10}$	20	(68.63)	NO	-	0.82	0.66±0.04
	40	(69.92)	NO	-	0.84	0.73±0.03
	50	(72.14)	NO	-	0.88	0.70±0.01
	55	(73.34)	NO	-	0.89	0.64±0.03
	59	74.68	Region the INA transition point		0.86	0.55±0.02
	60	75.19			0.88	0.54±0.03
	65	76.48	75.62	0.86	0.86	0.51±0.03
	70	78.55	76.90	1.65	0.88	0.69±0.04
	80	82.07	79.02	3.05	0.89	0.73±0.04

BMOAB	4-n-butyl-4-methoxyazoxybenzene
$\overline{6}O\overline{8}$	4-n-hexyloxyphenyl-4-n-octyloxybenzoate
$\overline{6}O\overline{10}$	4-n-hexyloxyphenyl-4-n-dexyloxybenzoate
$\overline{6}O\overline{6}NO_2$	4-n-hexyloxyphenyl-4-n-hexyloxynitrobenzoate
$\overline{8}CB$	8-cyanobiphenyl
$\overline{9}CB$	9-cyanobiphenyl

---

[1] γ_W, γ_A—for the vertical polarization of the incident beam and horizontal polarization of the scattered light.

[2] The temperature of the nematic–smectic C transition.

[3] The temperature of the NAC transition point.

tering intensity I given by

$$I = \frac{I(\pi/2)}{I_0(0)} \tag{3}$$

where $I(\pi/2)$ is the intensity at the scattering angle $\theta = \pi/2$, and $I_0(0)$ is the intensity of the laser beam transmitted through the sam-

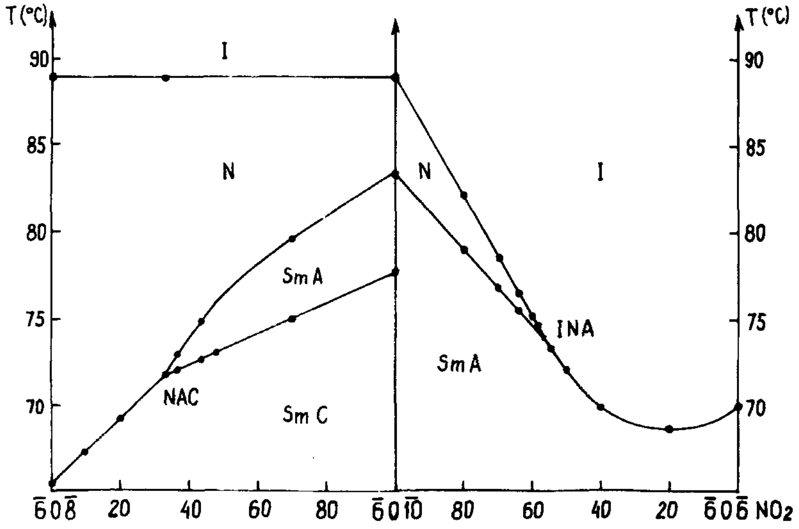

Mol. % $\overline{6}0\overline{10}$

FIGURE 2 Phase diagrams of the mixtures $\overline{6}0\overline{8}/\overline{6}0\overline{10}$ and $\overline{6}0\overline{10}/\overline{6}0\overline{6}NO_2$.

ple. The polarization plane of the incident beam was vertical. Both polarized and depolarized components of the scattered light were measured. The data fitting was carried out with the empirical formula

$$\frac{T}{I} = At^{\gamma} \tag{4}$$

where γ is an effective exponent which characterizes the curvature of $I^{-1}(t)$, $t = (T - T^*)/T^*$. The temperature dependence I^{-1} represented in Figure 3 as well as the results of the fit (Table I) demonstrate that the Curie-Weiss law is violated in all investigated liquid crystals and their mixtures regardless of the existence of smectic or nematic phases. Moreover the curvature increases while approaching the transition point.

There is a non-trivial question: how to compare the deviations from the linear dependence to each other. One can merely compare the deviations at the same distances from the transition point for the different substances.[9] But this way is not quite correct. The first order character of the I–N and I–A transition varies for different liquid crystals. For instance it is much stronger for $\overline{6}0\overline{6}NO_2$ than $\overline{6}0\overline{10}$. Therefore the different samples are at different distances from the absolute stability limit of the isotropic phase while approaching the transition point. The relative departures of the experimental data from *At* are

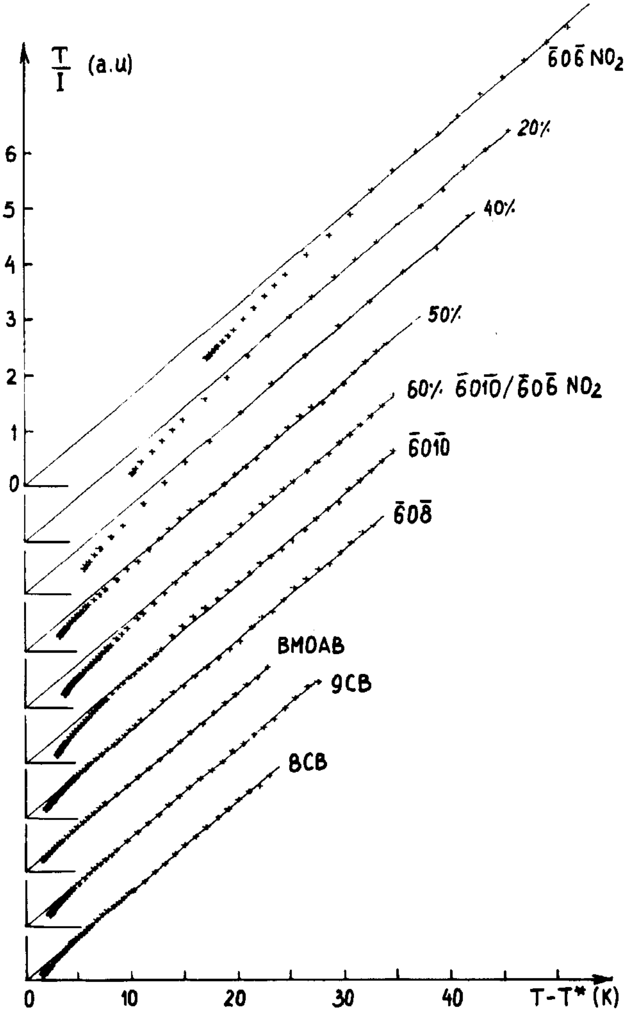

FIGURE 3 Inverse light-scattering intensity of the set of the liquid crystals and their mixtures.

shown in Figure 4. One can see that the effective departures at the same distance from T increases when one moves from the pure $\overline{6}0\overline{10}$ to pure $\overline{6}0\overline{6}NO_2$. Indeed, there is a suspicion that the temperature dependence of the intensity curves over the entire experimental range of temperature. The data were fitted by Eq. (4) in two temperature ranges: a) "wide range" is $t \approx 0.01$ to 0.1, b) "asymptotic range" is $t \lesssim 0.01$. The effective exponents are shown in Table I and Figure

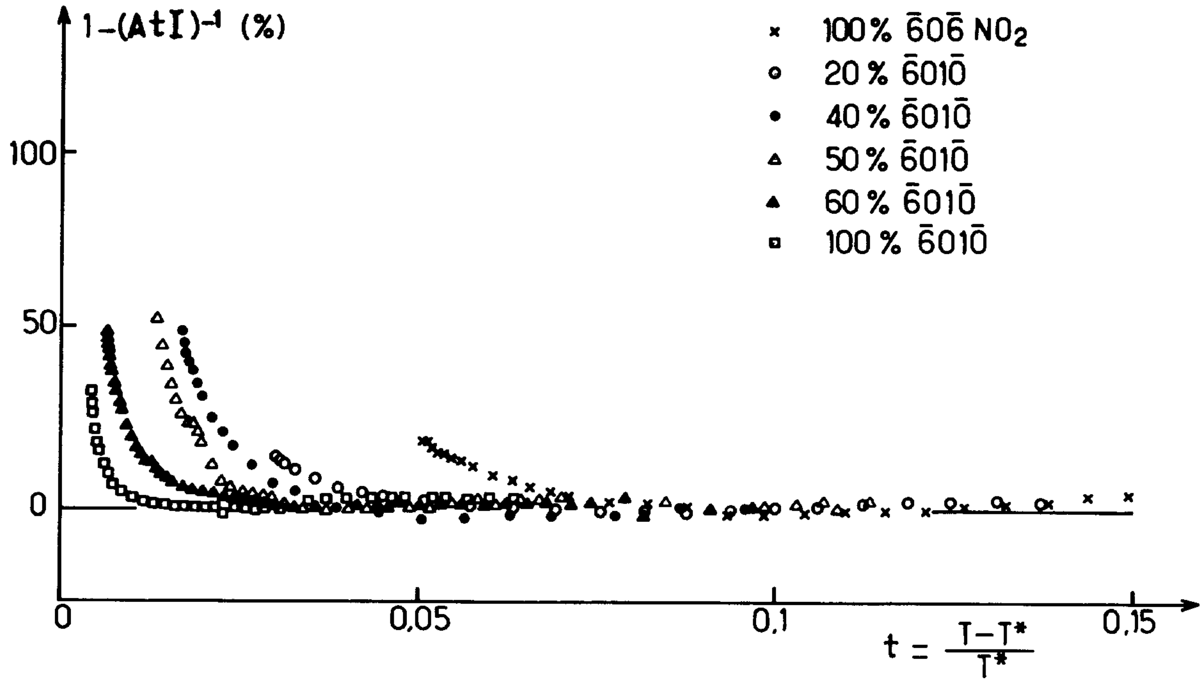

FIGURE 4 Relative deviations of the inverse intensity from the linear law.

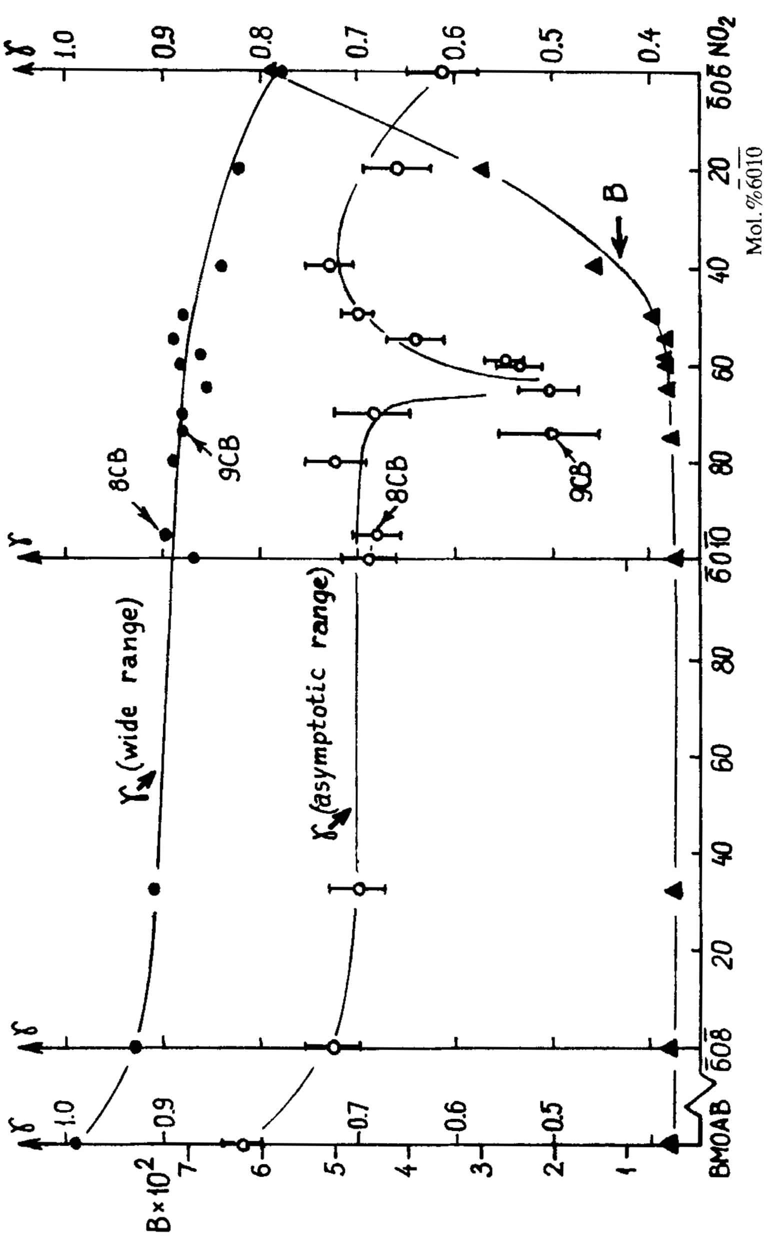

FIGURE 5 Effective curvature (circles) of the temperature dependence of the inverse intensity and the first-order power [B = $((T_{IN(IA)} - T^*)/T^*)^\gamma$] of the I–N and I–A transitions (triangles) in the set of the liquid crystals and their mixtures.

5. The value of γ in the "wide range" for the liquid crystals with various nematic ranges changes slightly and it is about 0.9. But the result of data fitting in the "asymptotic range" exhibits the influence of the smectic phase. The effective exponent γ has a sharp minimum close to the INA point for the mixture $\overline{6}0\overline{6}NO_2/\overline{6}0\overline{10}$. The effective exponents of 8CB and 9CB are close to those of the mixture $\overline{6}0\overline{6}NO_2/\overline{6}0\overline{10}$ at the same nematic ranges. The value of the scattering intensity at the transition points, normalized to the amplitude A is also shown in Figure 5.

It characterizes the first-order "power" of the transition. We can see from the figure that this value (B) increases rapidly for the I–A transition upon moving away from the INA point. The experimental data for the crystals with narrow nematic range are qualitatively described in the framework of the theory of a coupling between the nematic and smectic fluctuations.[11,12] We have performed the data fitting by the simplified equation (2) taking into account the main

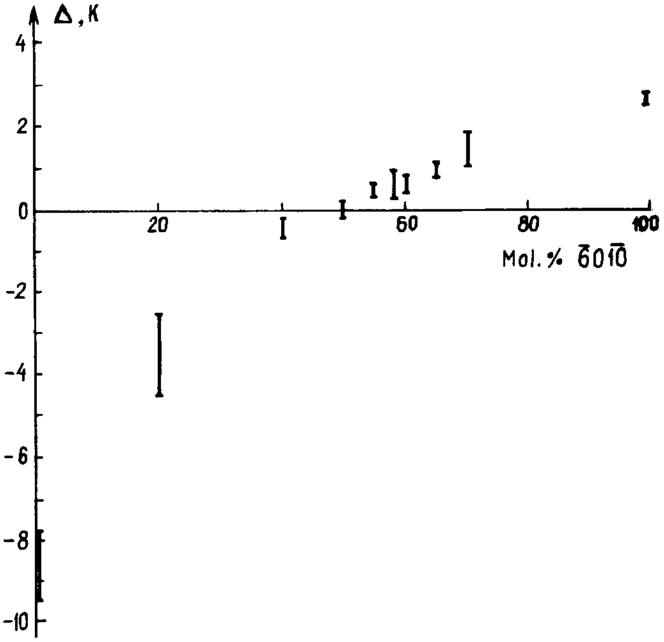

FIGURE 6 The evolution of the nematic–smectic gap in the $\overline{6}0\overline{10}/\overline{6}0\overline{6}NO_2$ mixture.

correction term:

$$\frac{T}{aI} = \frac{T - T^*_{IN}}{T^*_{IN}} - \frac{\tilde{B}^2_{NS} \, T^{*\,3/2}_{IN}}{(T - T^*_{IN} + \Delta)^{3/2}} \tag{6}$$

where $\Delta = T^*_{IN} - T^*_{IS}$.

This physically justified equation satisfies the experimental data in all temperature ranges. It has an obvious advantage as compared to the empirical formula (4) in which the effective exponent γ is really dependent upon temperature. In Eq. (5) $\tilde{B}_{NS}$ determines the magnitude of the deviations from the linear law while $T - T^*_{IN} + \Delta$ characterizes the increase of the curvature upon approaching the transition point. The smaller Δ, the larger the curvature. The evolution of the parameter Δ for the $\bar{6}0\bar{6}NO_2/\bar{6}0\bar{1}0$ mixture is shown in Figure 6. One can note that the region of the small values of Δ corresponds to the small values of γ (see Figure 5). It is remarkable that negative values of Δ were obtained for the I–S transition, and means that the bare absolute stability limit of the isotropic phase for I–S transition is higher than that for the I–N one. The data analysis performed above is reliable only if all distortion factors are taken into account. The major of them are the multiple and background scattering. The estimates made by the method proposed in Ref. 6 and our additional measurements in the small cell (optical path is 0.3 cm) show that the contribution of multiple scattering is comparable to experimental error (~1%). The Ornstein-Zernike corrections have the same order of magnitude.

The role of the background scattering can be revealed by the study of the depolarization ratio $\Delta_v \cdot \Delta_v$ changes upon approaching the transition point having the theoretical limit of 0.75 (Figure 7). The departures from the value of 0.75 far from the transition can be explained mainly by the isotropic scattering. We found an interesting and not quite understandable fact: this departure is larger for the samples with the narrow nematic range than for those without it.

Study of micellar solutions

Solutions of surfactants exhibit a rich variety of lyotropic phases. The micellar phase is the simplest example of such phases. Many nonionic aqueous amphiphilic systems have a low consolution point (so called "cloud point"). The problem concerning the nature of the cloud point in view of the universality conception of critical phenomena is so far unsolved.[13–15]

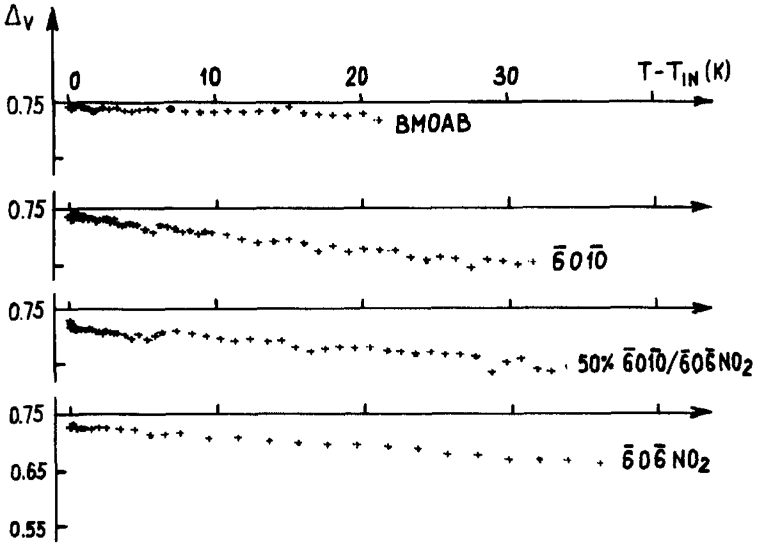

FIGURE 7 Temperature dependence of the depolarization ratio (Δ_v) for liquid crystals with different nematic ranges.

We performed the preliminary study of the critical opalescence in the aqueous micellar solution polyethyleneglycol-600-monolaurate. The commercial amphiphile with a large polydispersity was used. Both the relative scattering intensity and the autocorrelation function were measured at the scattering angle $\pi/2$. The phase diagram is shown in Figure 8. The point at which the consolution temperature T_S practically coincides with T* (the extrapolated absolute stability limit of the homogeneous phase) was considered to be a critical one. The critical point is displaced with respect to the minimum of the curve to the large amphiphile concentration. Probably, it is caused by the amphiphile polydispersity. The temperature dependence of the inverse light-scattering intensity is shown in Figure 9. The data fit by formula (4) gave the value of the effective exponent $\gamma \approx 1.2$ except for the immediate vicinity of the transition where the Ornstein–Zernike corrections as well as the multiple scattering were significant.

The temperature dependence of the diffusion coefficient obtained from the dynamic light-scattering autocorrelation function measurements is shown in Figure 10. The polydispersity analysis of the autocorrelation function in all investigated temperatures demonstrates the best fit for the single-exponent model. It means that in spite of

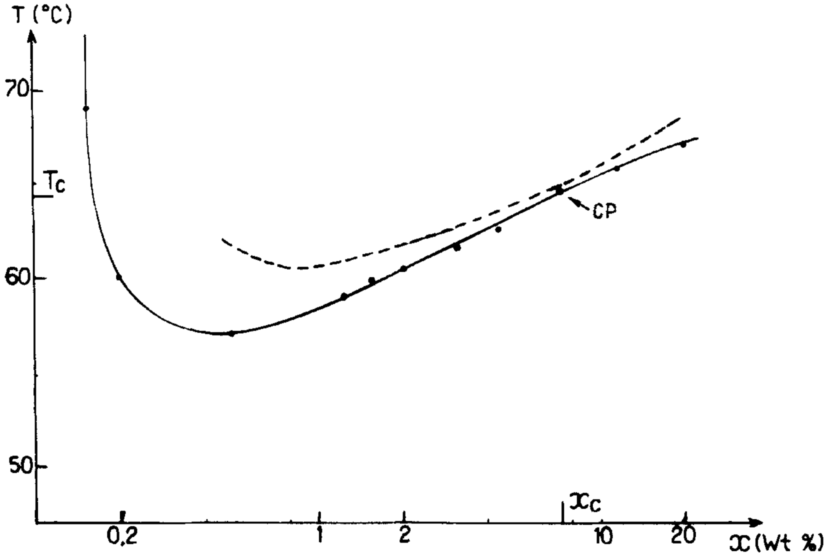

FIGURE 8 Phase diagram of the aqueous solution of PEG 600 monolaurate. Solid curve is the phase separation. Dashed curve is the absolute stability limit of the homogeneous phase.

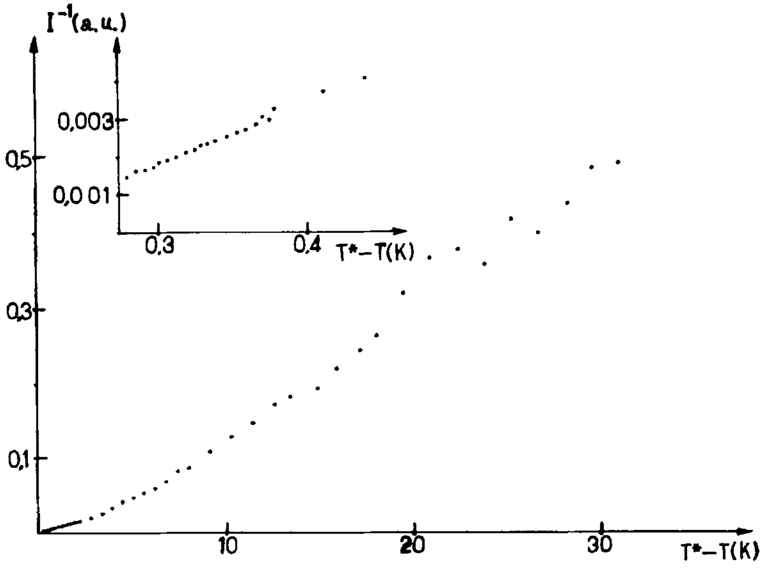

FIGURE 9 Temperature dependence of the inverse light-scattering intensity of the critical micellar solution.

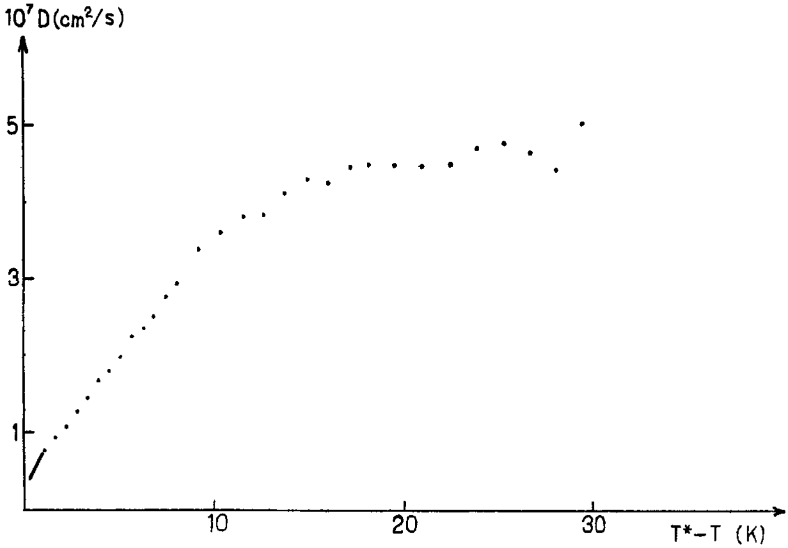

FIGURE 10 Critical slow down in the micellar solution. D is the hydrodynamic mass-diffusion coefficient.

polydispersity of the amphiphile there exists the single time of critical slow down and hence the single characteristic length as in ordinary binary mixtures.

References

1. L. D. Landau and E. M. Liftshitz, *Statistical Physics* (Pergamon) (1969).
2. P. C. De Gennes, *The Physics of Liquid Crystals*, Oxford (Clarendon) (1974).
3. T. W. Stinson and J. D. Litster, *Phys. Rev. Lett.*, **25**, 503 (1970).
4. T. W. Stinson, J. D. Litster and N. A. Clark, *J. de Physique*, **33**, 69 (1972).
5. C. P. Fan and M. J. Stefen, *Phys. Rev. Lett.*, **25**, 500 (1970).
6. L. V. Adzhemyan, L. T. Adzhemyan, A. Y. Valkov, L. A. Zubkov, I. V. Melnik and V. P. Romanov, *JETP*, **87**, 1244 (1984).
7. H. J. Coles and C. Strazielle, *Mol. Cryst. Liq. Cryst.*, **55**, 23 (1979).
8. A. Gohin, Thèse de spécialité, N_0 Bordeaux 1487 (1979).
9. H. Zink and W. H. de Jeu, *Mol. Cryst. Liq. Cryst.*, **124**, 287 (1985).
10. M. A. Anisimov, V. I. Labko, G. L. Nikolaenko and I. K. Yudin, *Mol. Cryst. Liq. Cryst. Lett.*, **2**, 77 (1985).
11. A. Gohin, C. Destrade, Gasparoux and J. Prost, *J. de Phys.*, **44**, 427 (1983).
12. M. A. Anisimov, E. D. Gorodetskii and V. E. Podnek, *JETP Letters*, **37**, 414 (1983).
13. M. Corti, C. Minero and V. Degiorgio, *J. Phys. Chem.*, **88**, 309 (1984).
14. L. J. Magid, R. Triolo and J. S. Johnson, *J. Phys. Chem.*, **88**, 5730 (1984).
15. M. Corti and V. Dgiorgio, *Phys. Rev. Lett.*, **55**, $N_0$19, 2005 (1985).